



**Cationic Poly-Amido-Saccharides: Stereochemically-defined,
Enantiopure Polymers from Anionic Ring-opening
Polymerization of an Amino-Sugar Monomer**

Journal:	<i>Polymer Chemistry</i>
Manuscript ID	PY-ART-11-2019-001691.R2
Article Type:	Paper
Date Submitted by the Author:	24-Jan-2020
Complete List of Authors:	Balijepalli, Anant; Boston University, Dept of Biomedical Engineering + Chemistry Hamoud, Aladin; Boston University, Dept of Biomedical Engineering + Chemistry Grinstaff, Mark; Boston University, Dept of Biomedical Engineering + Chemistry

ARTICLE

Cationic Poly-Amido-Saccharides: Stereochemically-defined, Enantiopure Polymers from Anionic Ring-opening Polymerization of an Amino-Sugar Monomer

Received 00th January 20xx,
Accepted 00th January 20xx

DOI: 10.1039/x0xx00000x

Anant S. Balijepalli,^{*a} Aladin Hamoud^b and Mark W. Grinstaff^c

Efforts to develop synthetic carbohydrate polymers, despite their potential uses in biomedical applications, lag behind those of synthetic polypeptides and polynucleotides due to their structural complexity and the challenging methods associated with their synthesis. While carbohydrate polymers with functional groups such as carboxylic acids (alginate) and amines (chitosan) are used as hydrogels and nanocarriers for therapeutics, the potential for contamination, batch-to-batch variation, and poor chemical definition limits their translation to clinical application. Inspired by these challenges, we describe efforts towards the design and synthesis of enantiopure, amine-functional carbohydrate polymers with defined stereochemistry, narrow molecular weight distributions, helical conformations, water solubility, and degrees of polymerization up to 50. Multiple synthetic routes are described, along with their limitations, to highlight the role of protecting group choices in the successful development of these polymers.

Introduction

Carbohydrate polymers are one of the three major classes of biopolymers found in all organisms, along with polypeptides and polynucleotides.¹ While the discovery of biological and synthetic tools to manipulate polypeptides and polynucleotides such as proteases², restriction enzymes³, cloning⁴, and solid phase synthesis^{5,6} have led to numerous biomedical advances as well as a widespread appreciation for their utility, efforts to synthesize and apply carbohydrate polymers lag behind due to the inherent complexity of these systems^{1,7–10}. Unlike polypeptides and nucleic acids, which vary in functionality at a single position with identical stereochemistry and are usually linked linearly, carbohydrate polymers differ in functionalities, stereochemical configuration, and degree, stereochemistry, and regiochemistry of branching per monomer unit^{8–10}. These structural and functional variations significantly impact their macromolecular chemical, physical, and biological properties, and as a result, are vital considerations in biomedical applications^{8,10,11}. Additionally, such chemical diversity presents an obstacle for their extraction from natural sources as methods to isolate polysaccharides often yield products contaminated with chemically similar polysaccharides^{12–14} as well as products with poorly defined molecular weight distributions^{15–17} that are challenging to further purify. Additionally, synthetic efforts toward carbohydrate polymers

must account for other challenges including the presence of multiple nucleophilic hydroxyl groups^{7,9–11}, retention of stereochemistry at each position^{9–11}, and the anomeric effect that leads to an α -favored α/β mixture at the C1 position¹⁸. To address these limitations, chemists are precluded from using many synthetically useful transformations^{1,8,9,11} and often utilize extensive protecting group strategies^{1,7,9,11}. The associated time, and reduction in yield, while applicable to oligomers, are prohibitive for the synthesis of carbohydrate polymers ($n \geq 25$)¹⁹.

As carbohydrates play a wide range of biological roles from metabolism and energy storage to cell-cell recognition, there is a high demand for their unique properties in biomedical applications^{1,7,8,10,11}. Given the relative difficulty in obtaining enantiopure and high molecular weight synthetic carbohydrate polymers^{10,20,21}, existing literature related to carbohydrate polymers primarily addresses either naturally obtained polysaccharides²² or synthetic linear backbone polymers (acrylates, carbonates, esters) grafted with saccharide moieties (i.e., glycomaterials)^{8,23–25}. For example, heparin sulfate, alginate²⁶, hyaluronic acid²⁷, and chitosan²⁶ are prime examples of polysaccharides widely utilized in biomaterial formulations such as hydrogels²⁸ and nanoparticles²⁹ in order to improve bioactivity, hydrophilicity, and shielding from immune clearance. These results, while encouraging, involve materials that may be contaminated by chemically similar material^{13,14}, display significant batch-to-batch variation^{30,31}, and possess poorly defined molecular weight distributions^{15–17}. In response to the need for mild, reliable, and facile methods to synthesize carbohydrate polymers, our group reported new materials derived from glucose and galactose termed Poly-Amido-

^a Department of Biomedical Engineering, Boston University, Boston, MA, 02215

^b Department of Chemistry, Boston University, Boston, MA, 02215

^c School of Medicine, Boston University, Boston, MA, 02218

Electronic Supplementary Information (ESI) available: Small molecule synthetic procedures, supplementary figures, NMR, MS, and IR spectra. See DOI: 10.1039/x0xx00000x

Saccharides (PAS)^{20,32,33}. Unlike other recently reported carbohydrate-mimic polymers and glycopolymers that are either completely insoluble in water^{34–39} or comprised of linear aliphatic backbones with pendant monosaccharides⁴⁰, PAS closely resemble natural polysaccharides by possessing a backbone comprised of rigid pyranose rings, enantiopurity, biocompatibility, hydrophilicity, dense hydroxyl functionality, and can be obtained with molecular weights exceeding 10 kDa³². In contrast to natural polysaccharides, however, PAS are linked by an α -1,2-amide bond that confers advantageous hydrolytic resistance and are obtained pure with a well-defined molecular weight distribution^{20,32,33}. Our recently reported PAS polymers resemble natural polysaccharides functionalized by hydroxyl groups, such as dextran, amylose, and glycogen that are largely associated with metabolic and structural roles^{20,32,41}. Introducing functionality to glucose-based PAS via lipid initiating groups or co-polymerization with a L-lysine- β -lactam monomer has led to potent inhibitors of biofilm formation⁴² and antimicrobial agents⁴³. Thus, the synthesis of functionalized or reactive PAS polymers will afford new compositions for study and insights into the limitations of the polymerization reaction, as well as widen the application space of PASs to mimic additional polysaccharides.

We are particularly interested in developing a regioselectively functionalized PAS polymer based on an amino sugar repeating unit due to the widespread application of chitosan-based materials as mucoadhesives⁴⁴, drug carriers²⁹, and nucleic acid vectors⁴⁵ (Chart 1). We recently communicated a PAS with regioselectively introduced 6-amino functionality (AmPAS) and our preliminary data indicate that these polymers are biocompatible and mucoadhesive, as expected⁴⁶. The synthesis of these polymers, however, required significant optimization due to the competing requirements of stability towards monomer synthesis and polymerization in addition to simple deprotection. Herein, we complement our previously reported work by providing a detailed account of the strategy, synthetic efforts, and successes (as well as failures) to AmPAS including: 1) identification of bicyclic candidate monomers; 2) anionic ring opening polymerization of these monomers and the dependence of the amine protecting group (e.g., Boc, Nosyl, Phth, Tosyl) on polymerization; 3) deprotection routes to the desired polymers; and, 4) physicochemical characterization of the resulting amino poly-amido-saccharides. The findings presented exclusively herein inform the synthesis of other functionalized PAS by identifying optimal routes for regioselective transformation and the scope of the [2+2] cycloaddition monomer synthesis. Additionally, our data provide guidance for the synthesis of other cationic β -peptide polymers by anionic ring opening polymerization by identifying suitable amine protecting groups.

Experimental methods

Small molecule synthetic methods

We prepared the small molecule glycals **12**, **14**, **16**, **18**, and **19** as described in the Supplementary Information. All reactions

were performed on the multi-gram scale and yields were good to excellent.

NMR cycloaddition reactions

Glycals **12**, **14**, **16**, and **18** were dissolved to 0.5 M in 400 μ L from a fresh glass ampule of CD₃CN (0.2 mmol). Trichloroacetyl isocyanate (2.0 eq, 50 μ L, 0.4 mmol) was quickly added to the solution, the time was noted, and the mixture was transferred to an NMR tube. ¹H-NMR experiments were performed at time points distributed over 48 hours; the peaks corresponding to starting material, [4+2] product, and [2+2] product were clearly separated and quantifiable. The relative ratio of starting material in the reaction mixture was calculated as a fraction of the peak areas of all 3 major reaction components. Although some byproducts were observed, these peaks comprised a negligible portion of the total integral and the ratio between the peak intensities of [4+2], [2+2], and these impurities remained constant over the experiment period. The logarithm of the ratio of starting material present in the mixture was plotted against time and linearly fit to extract the slope (reaction rate constant).

Synthesis of protected AmPAS

Freshly distilled THF was degassed with argon for 30 minutes while simultaneously evacuating and re-filling a Schlenk flask loaded with 3 Å molecular sieves under argon. LiHMDS was obtained from a glove box and a solution was prepared using the freshly-degassed THF (solution was stable for >12 h with no color / oxidation visible). A solution of initiator (4-*tert*-butylbenzoyl chloride) was prepared using this freshly-degassed THF. Monomer **20** was weighed out (200 mg, 0.427 mmol), dissolved in 3 mL of degassed THF, and added to the Schlenk flask. The reaction mixture was cooled to 0 °C and the appropriate amount of initiator (2 mol % for 50-mer, 4 mol % for 25-mer, 8 mol % for 12-mer) was added (calculated to be 500 μ L) via a glass syringe to the Schlenk flask. After 10 minutes, 2.5 eq of LiHMDS to the initiator (3.5 eq for monomer **17**) was added (also calculated to be 500 μ L for ease of measurement) via glass syringe to the Schlenk flask quickly. The reaction mixture developed a yellow color and, after 30 minutes, the ice bath was removed to allow the reaction to warm to room temperature. The reaction was then monitored by TLC for starting material consumption (permanganate stain, UV, TLC). The solvent was removed from the reaction mixture by rotary evaporation and the residue was dissolved in DCM,

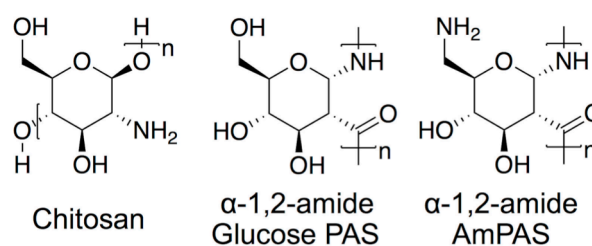


Chart 1. Comparison of repeating unit structures of Chitosan, previously reported α -1,2-amide glucose-PAS, and α -1,2-amide AmPAS.

washed with 1 M HCl, saturated bicarbonate, brine, dried over sodium sulfate, and evaporated to dryness. The crude residue was dissolved in a minimum amount of DCM and added dropwise to a stirring, ice-cold solution of pentane. The precipitate was obtained via filtration and air-dried followed by vacuuming drying to yield **PB''** as a white powder. (Yields 75-82%, 150-164 mg). $^1\text{H NMR}$ (500 MHz, CDCl_3) δ 8.21-7.80 (br), 7.55-6.55 (br), 6.21-5.10 (br), 5.08-3.88 (br), 3.88-2.46 (br), 1.63-0.96 (br). SEC (THF) $M_w = 6.8$ kDa, $M_n = 6.0$ kDa, $D = 1.1$.

AmPAS deprotection and isolation

Polymers **PB''** (150 mg, 0.32 mmol repeating unit) were dissolved in 4 mL of DCM, and 2 mL of TFA was added to the stirring solution (due to TFA fumes, the reactions were conducted in glass vials and covered with glass stoppers). The reaction was allowed to proceed for 4 hours and the solvent was then removed by rotary evaporation. The residual TFA was removed by repeatedly adding DCM, dissolving the contents of the flask, and evaporating the mixture. After three of these rounds of evaporation, a sticky solid residue was obtained. To this residue was added 2 mL of 1 M NaOH and 2 mL of DCM and the mixture was vigorously dissolved with vortexing. More 1 M NaOH and DCM was added in a 1:1 ratio until the total solution volume reached 8 mL to aid in dissolving the crude residue. Then, the mixture was diluted with 8 mL of DCM and washed 4 times with 4 mL of 0.1 M NaOH. The combined aqueous washes were back-extracted with 4 mL of DCM and this was added to the organic extracts. 4 mL of a 0.1 M NaOH / brine solution was added to the vial and, after washing, the organic layer was transferred to a fresh vial and sodium sulfate was added. The mixture was then filtered (and previous vials rinsed thoroughly with DCM) and the solvent was removed under rotary evaporation. A 250 mL tri-neck flask was equipped with a glass stir bar and condenser and was cooled to -63 °C (condenser was cooled to -78 °C). The flask was connected to an anhydrous NH_3 tank and 100 mL of the gas was allowed to condense over 30 minutes while stirring. While ammonia was condensing, freshly distilled THF was degassed with argon for 30 minutes while simultaneously aliquoting LiHMDS from a glove box. The crude residue was then dissolved in 2 mL of freshly degassed THF in a vial equipped with a stir bar, while LiHMDS was dissolved to form > 1 mL of a 1 M solution. Sodium metal was cut in cyclohexane and added to the liquid ammonia to generate a deep blue-colored solution, followed by the addition of 3.0 eq of LiHMDS (vs. repeating unit, 960 μL , 0.960 mmol) to the THF solution of crude residue with vigorous stirring. The mixture of LiHMDS and crude product formed a bright red color, and the solution was transferred dropwise to the flask with liquid ammonia. The reaction was allowed to proceed for 45 ($[\text{M}]_0/[\text{I}] = 12$), 60 ($[\text{M}]_0/[\text{I}] = 25$), 90 ($[\text{M}]_0/[\text{I}] = 50$), or 120 minutes ($[\text{M}]_0/[\text{I}] = 100$) and a saturated solution of NH_4Cl was added dropwise to quench the reaction. The resulting clear solution was allowed to evaporate overnight while stirring to yield a white solid or a white paste. This white residue was dissolved in water and extracted twice with diethyl ether. The aqueous layer was then

added to 1 kDa MWCO dialysis tubing and dialyzed overnight (changes at 4, 8, and 16 h). The contents of the dialysis bag were recovered after 24 h, passed through a 0.45 μm syringe filter, and lyophilized over 3 days to obtain **P1-3** as a white, cotton-like, fluffy solid. (Yield 46-79% over two steps, 28 mg **P1**, 47 mg **P2**, 43 mg **P3**). $^1\text{H NMR}$ (500 MHz, D_2O) δ 5.68-5.38 (bm, 1H, H1), 3.98-3.60 (bm, 1H, H4), 3.46-3.25 (bm, 1H, H3), 3.21-2.66 (bm, 3H, H5, H6-1, H6-2). $^{13}\text{C NMR}$ (126 MHz, CDCl_3) δ 169.43 (NHCO), 74.40 (C1), 71.83 (C5), 76.14 (C3), 69.80 (C4), 51.49 (C2), 40.34 (C6). SEC (H_2O , 0.1 M AcOH, 0.02 M glycine, pH 2.3) $M_w = 4.7$ kDa, $M_n = 4.1$ kDa, $D = 1.1$.

Size exclusion chromatography

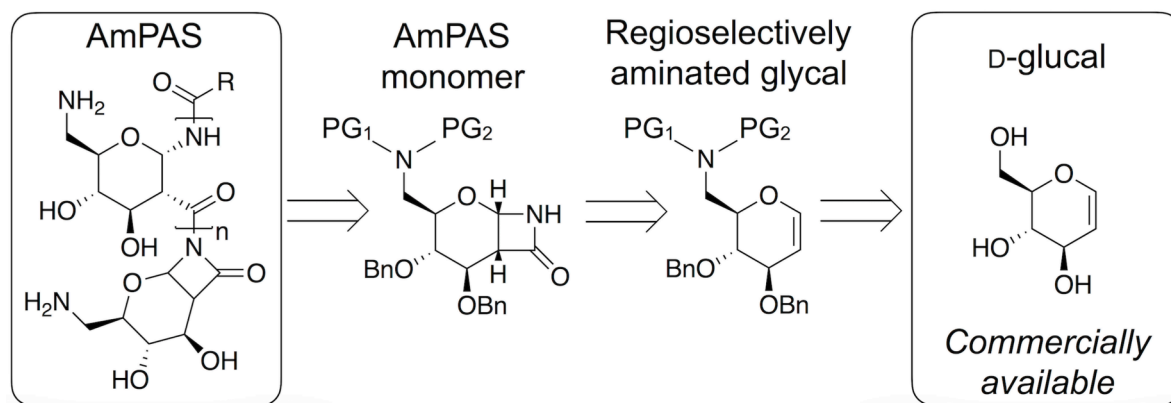
Protected polymer molecular weights were determined by size exclusion chromatography (SEC) versus polystyrene standards using THF as the eluent at a flow rate of 1.0 mL/min through two Jordi columns (Jordi Gel DVB 105 Å and Jordi Gel DVB 104 Å, 7.8 x 300 mm) at 25 °C in series with a refractive index detector. All calculations were performed using Breeze GPC software (Waters, Milford, MA). Deprotected polymer molecular weights were determined by aqueous GPC versus poly(2-vinylpyridine) standards using aqueous buffer (0.1 M AcOH, 0.02 M glycine, pH 2.3) as the eluent at a flow rate of 0.5 mL/min through two PL aquagel columns (OH 60 micron, 7.8 x 300 mm) at 25 °C in series with a refractive index detector. All calculations were performed using Cirrus GPC software (Agilent, Santa Clara, CA).

Polymerization kinetics

Monomer **20** (100 mg, 0.213 mmol) was added to 2 mL of freshly degassed THF while stirring at 0 °C as previously described with $[\text{I}] = [\text{M}]_0/25$. After 10 minutes, LiHMDS (2.5x $[\text{I}]$) was added quickly to the reaction and a timer was simultaneously started. 100 μL was removed from the reaction at 20, 40, 60, 90, 120, 180, 240, 300, 1800, and 3600 s and quickly injected into a saturated aqueous solution of NH_4Cl to quench the reaction. The quenched reactions were diluted with DCM, washed with 0.1 M HCl, saturated bicarbonate, brine, dried over sodium sulfate, and evaporated to dryness. Residues were transferred to HPLC vials and reconstituted in exactly 1 mL THF for SEC analysis using THF as the eluent and polystyrene standards. Chromatograms typically consisted of one lower retention time peak (polymer chain) and one higher retention time peak (monomer) that was outside the calibration curve range.

Circular dichroism

Circular dichroism (CD) studies were performed in a 1 mm path length cuvette using an Applied Photophysics CS/2 Chirscan with a standard Mercury lamp. Polymers were dissolved in water (2 mg/mL) and diluted in the appropriate mixture of buffer and water to a final concentration of 0.2 mg/mL for CD analysis. Measurements with polymers of different length, with varying temperature, and with varying salt concentration were performed using the buffer for pH 7 (phosphate buffer w/o chloride). Measurements at pH 3 were conducted with phosphate buffer w/o chloride and



Scheme 1. Retrosynthetic scheme of amine-functional PAS (AmPAS) from the commercially available D-glucal highlighting the key intermediates: 1) regioselectively amine-functionalized glycol and 2) di-protected AmPAS monomer with suitable stability for polymerization and deprotection.

measurements at pH 9 were conducted with borate / NaOH buffer.

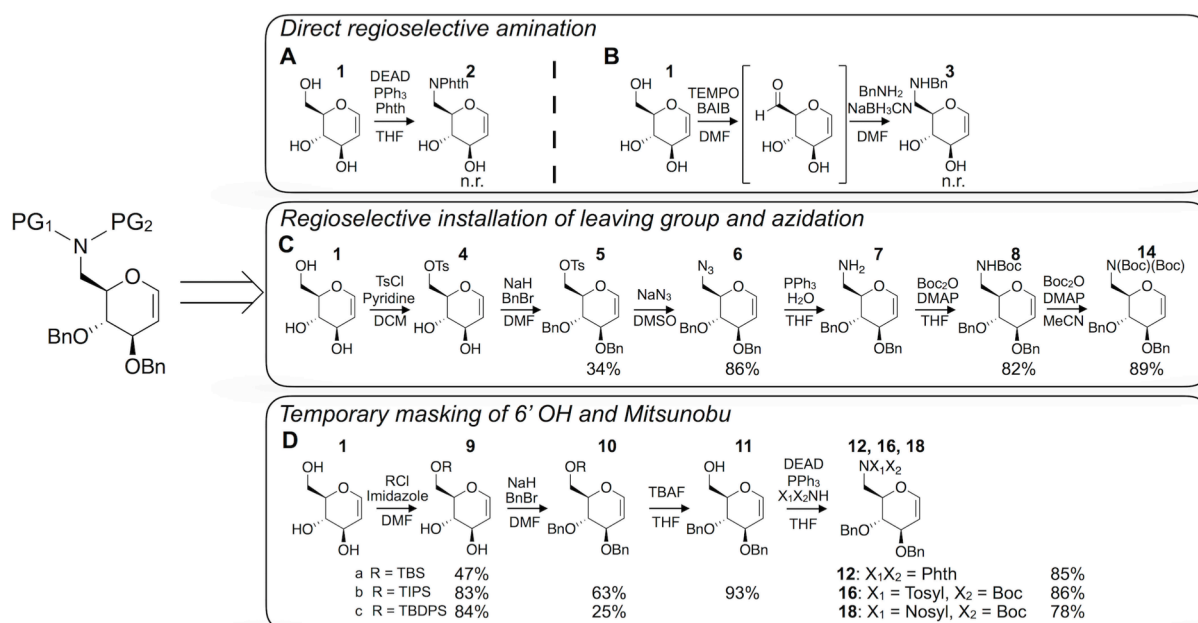
Results and Discussion

We reported the synthesis of glucose- and galactose-derived PAS in three steps from the commercially available tri-*O*-benzyl-D-glucal and tri-*O*-benzyl-D-galactal²⁰. First, these protected glycol structures underwent a [2+2] cycloaddition reaction with chlorosulfonyl isocyanate (CSI), followed by an *in situ* reduction by sodium bis(2-methoxyethoxy)aluminum hydride (Red-Al) to yield a tri-*O*-benzyl protected bicyclic sugar-β-lactam. The lactam was then polymerized via anionic ring opening polymerization (AROP) catalyzed by the sterically hindered strong base Lithium bis(trimethylsilyl)amide (LiHMDS), which also stoichiometrically participates in the *in situ* reaction of an activated carbonyl and monomer to form the

initiator. After polymerization, a Birch-type reduction globally deprotected all *O*-benzyl groups and subsequent dialysis and lyophilization afforded the PAS²⁰. Through judicious selection of an appropriately regioselectively 6-amine-functionalized protected glycol, we hypothesized that a similar approach would translate to the synthesis of AmPAS (Scheme 1).

Identifying a suitable strategy for regioselective amine functionalization

As shown in Scheme 2, we identified four strategies to regioselectively modify the commercially available D-glucal (**1**). Strategies 2A and 2B, involving the direct regioselective Mitsunobu reaction and reductive amination of the 6' OH respectively, presented the most direct routes to the desired amine-modified glycol. In Scheme 2A, Mitsunobu reactions in



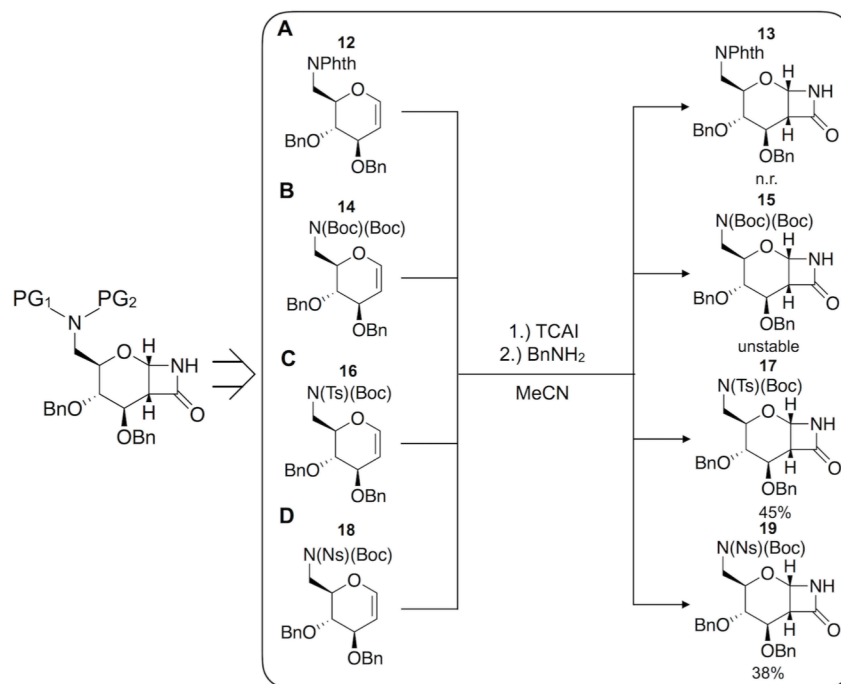
Scheme 2. (A-D) Retrosynthetic design for di-protected amine-functionalized glycols starting from commercially available D-glucal. See ESI for detailed synthetic methods for the synthesis of glycols **4-12**, **14**, **16**, and **18**.

DMF and DMF/THF mixtures using both diphenylphosphoryl azide (DPPA) and phthalimide afforded degradation reactions as starting material is consumed in the absence of a formed glycal product (**2**) by TLC. Attempts to perform a one-pot reductive amination (Scheme 2B) by *in situ* oxidation of the 6' OH to the aldehyde by TEMPO followed by the addition of benzylamine and subsequent reduction by sodium cyanoborohydride (**3**) also led to degradation of the glycal by TLC. In Scheme 2C, we regioselectively installed a 6-*O*-tosyl group (**4**) with the goal of further reducing polarity via 3' and 4'-OH benzyl protection (**5**), followed by a nucleophilic displacement by sodium azide (**6**), subsequent Staudinger reduction (**7**), and *in situ* Boc protection (**8**). The 6-*O*-tosyl glycal, however, was highly unstable, and a previously reported intramolecular nucleophilic displacement reaction results in a considerable reduction in yield⁴⁷ and difficulty in product isolation by chromatography. To mitigate losses, the crude product of the tosylation reaction (**4**) was immediately carried on to benzyl protection. Nevertheless, isolated yields over these two steps were low (34%) prompting examination of other strategies. As an alternative, Scheme 2D utilized bulky silyl protecting groups (**9a**, **9b**, **9c**) to enforce regioselectivity, followed by benzyl protection (**10**) and subsequent fluoride-mediated deprotection to yield 3,4-di-*O*-benzyl-D-glucal (**11**). This method possessed several advantages including reagents compatible with the highly sensitive glycal alkene, significant polarity differences between starting materials and products for facile separation, and a final product useful for divergent synthesis. TBS, TIPS, and TBDPS protecting groups all readily formed the regioselectively-protected product with TBDPS protection affording the highest yield. This TBDPS-protected

glycal, however, suffered from diminished yields when carried forward to benzyl protection (25%), likely as a result of the additional steric hindrance. Utilizing TIPSCl for regioselective protection of the glycal 6'-OH, instead of TBDPSCl, afforded the desired product in the highest yield (49%) over all 3 steps.

Suitability of phthalimide amine protection to cycloaddition and polymerization

To convert the single hydroxyl group of 3,4-di-*O*-benzyl-D-glucal to a protected amine functionality in one step, we utilized the Mitsunobu reaction that was previously found to be unsuccessful. The Mitsunobu reaction is a powerful and well-studied transformation with clear limitations including the pKa requirement of the pro-nucleophile and the challenging separation of reaction products⁴⁸. Inspired by the Gabriel amine synthesis, the reaction was initially performed utilizing phthalimide as the nitrogen-containing pronucleophile, diethyl azodicarboxylate (DEAD), and triphenylphosphine in THF (Scheme 2D). We removed the resulting triphenylphosphine oxide by recrystallization from cold toluene and ether, and after chromatographic separation obtained an impure yellow solid product. Recrystallization from boiling isopropanol yielded the pure 3,4-di-*O*-benzyl-6-*N*-phthalimido-6-deoxy-D-glucal (**12**) in 85% isolated yield. The [2+2] cycloaddition reaction between this glycal and CSI, using previously reported conditions (Scheme 3A, -63 °C, 3 hours), did not proceed and only unreacted starting material could be isolated (~97% recovery). We repeated this reaction using higher temperatures (-55 °C, 4 hours; -40 °C, 4 hours) and in all cases only starting material was recovered from the reaction mixture. This result was extremely surprising, given the high reactivity of CSI with



Scheme 3. (A-D) Retrosynthetic design for di-protected β -lactam monomers from **12** (Scheme 2D), **14** (Scheme 2C), **16** (Scheme 2D), and **18** (Scheme 2D). See ESI for detailed synthetic procedures for **13**, **15**, **17**, and **19**. Briefly, all glycals were reacted with 4.0 eq of trichloroacetyl isocyanate (TCAI) for 2-7 days, followed by cooling to -30 °C and slow quenching with 4.4 eq of benzylamine.

enol ether glycols. Thus, we investigated another activated isocyanate (trichloroacetyl isocyanate, TCAI) to synthesize β -lactams from glycols, as previous literature reports indicated that the reaction proceeded under milder reaction conditions (20 °C, atmospheric pressure) that could be monitored by TLC^{49,50}. After performing this reaction to complete consumption of the phthalimide-protected glycol by TLC and subsequent removal of the *N*-trichloroacetyl group by benzylamine, we obtained only negligible quantities of the desired product. In order to determine if the glycol was being degraded, we performed NMR reactions in CD₃CN and showed that the reaction proceeded smoothly, albeit with a significantly slower rate compared to 3,4,6-tri-*O*-benzyl-D-glucal (Figure S1). The benzylamine used to remove the *N*-trichloroacetyl group, however, was sufficiently nucleophilic to attack and open the phthalimide group. Although the phthalimide group is stable to the reductive conditions utilized to remove the *N*-chlorosulfonyl group after the cycloaddition with CSI, the combination of long reaction times (>48 h) at low temperatures precluded the use of this protecting group in the monomer synthesis.

Suitability of *N*-boc and *N,N*-di-boc protection to cycloaddition and polymerization

To overcome these drawbacks, we next examined scheme 2C using the *N*-boc protected glycol for the [2+2] cycloaddition reaction. This glycol underwent a side reaction with TCAI (Figure S2), however the addition of a second boc group (**14**) allowed for a cycloaddition reaction (29% yield) with a similar rate constant observed for the phthalimide glycol (Figure S1). This lactam (**15**), (Scheme 3B) however, could not be isolated pure and failed to polymerize even with additional catalyst up to 5x [I], higher temperatures up to 50 °C, and longer reaction

times up to 24 hours.

Monomer synthesis and polymerization utilizing *N*-tosyl-*N*-boc protection

Given these challenges, we revisited the Mitsunobu reaction with an *N*-tosyl-*N*-boc protection combination in order to provide the necessary stability to survive both the cycloaddition and polymerization reactions while reducing some bulkiness to improve polymerizability. We isolated the product, 3,4-di-*O*-benzyl-6-*N*-tosyl-6-*N*-boc-6-deoxy-D-glucal (**16**), as an oil with minor impurities that could not be removed despite multiple chromatographic separations (Scheme 2D). Nevertheless, this glycol reacted with TCAI at a similar rate (Figure S1) to the phthalimide-protected glycol via NMR analysis. We obtained the desired lactam monomer product (**17**) in 48% yield

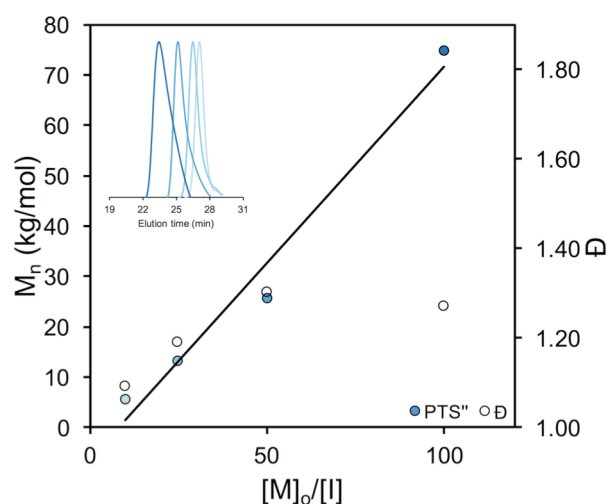
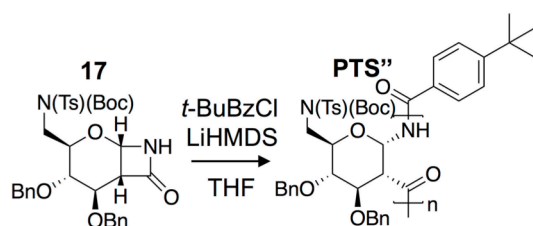


Figure 1. M_n vs. $[M]_0/[I]$ for PTS'' polymers (monomer **17**) indicates linearity up to $[M]_0/[I] = 100$ and dispersities remain under 1.3. Inset shows SEC chromatograms of polymers.



Scheme 4. Polymerization of monomer **17** (see methods): 4-*tert*-butylbenzoylchloride (I) is attacked by deprotonated monomer (M) to yield the initiating species. LiHMDS acts as stoichiometric base and polymerization catalyst.

Table 1. SEC characterization of PTS'' polymers obtained from polymerization of **17**.

Polymer	$[M]_0/[I]$	LiHMDS x [I]	$M_{n,theor}$ (kDa)	$M_{n,GPC}$ (kDa)	\mathcal{D}	Yield
PTS1''	10	2.5	6.2	5.61	1.1	70%
PTS2''	25	2.7	15.6	13.1	1.2	71%
PTS3''	50	3.0	31.1	25.5	1.3	65%
PTS4''	100	3.5	62.2	74.8	1.3	75%

(Scheme 3C) despite an equally favorable competing [4+2] cycloaddition reaction. Next, we polymerized (Scheme 4) **17** by addition of 4-*tert*-butylbenzoyl chloride, followed by LiHMDS to form the initiator *in situ*. The high reactivity of 4-*tert*-butylbenzoyl chloride is well established^{20,43} and we accordingly expected lower \mathcal{D} (< 1.3) when utilizing this reagent for the polymers reported in this manuscript compared to those previously reported using pentafluorophenyl *S*-benzylthioglycolate. Polymers with M_n ranging from 5.6 kDa to 74.8 kDa were obtained with isolated yields ~75% (Table 1, see methods for synthetic details). Size exclusion chromatography of these polymers, referenced to polystyrene standards, showed monomodal distributions with low \mathcal{D} . While the polymerization of this monomer was not completely inhibited by steric bulk, a higher catalyst loading (up to 3.5x $[M]_0/[I]$) was required to achieve complete conversion as indicated by TLC. Unfortunately, the Birch-type reduction to remove the *N*-tosyl and *O*-benzyl groups failed as the *N*-tosyl group remained even when performing the reaction at higher temperatures (-53 °C, -44 °C) or with alternative metal reductions (Mg/MeOH, Na/Anthracene, SmI₂/THF/H₂O).

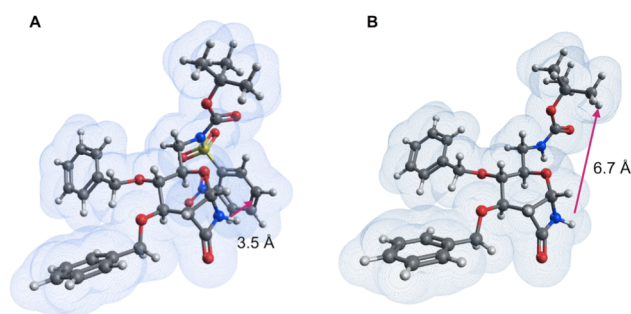
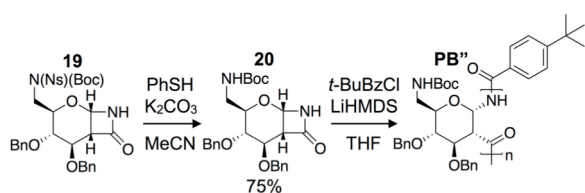


Figure 2. (A) Minimized structure (B3LYP/6-31G(d)) of monomer **19** displays steric hindrance at the lactam nitrogen. (B) Minimized structure of monomer (B3LYP/6-31G(d)) **20** displays significantly larger space available for polymerization.

Improving *N*-sulfonyl lability via nosyl protection

We subsequently identified the *N*-(2-nitrobenzenesulfonyl) protecting group as a promising candidate for the cycloaddition and polymerization reactions due to its intermediate stability between the *N*-phthalimide and *N*-tosyl protecting groups, lower bulk than the di-*N,N*-boc system, and appropriate pKa for the Mitsunobu reaction. The greater polarity of this product compared to the other systems increased the difficulty of separation after the Mitsunobu reaction (Scheme 3D), even when using alternative Mitsunobu reagents such as the water soluble di-2-methoxyethyl-azodicarboxylate (DMEAD). Despite these challenges, we successfully isolated the product as an oil, again with minor impurities, from a toluene/ethyl acetate purification system. The NMR cycloaddition reaction of this glycal with TCAI occurred with similar reaction times as the other amine-modified glycals. Once more, the monomer did not successfully polymerize, likely due to steric constraints. Unlike the *N*-tosyl protected lactam monomers (**17**), we removed the nosyl group without affecting the lactam using



Scheme 5. Nosyl deprotection of **19** via PhSH furnishes monomer **20** (see ESI). Polymerization of monomer **20** (see methods): 4-*tert*-butylbenzoylchloride (**I**) is attacked by deprotonated monomer (**M**) to yield the initiating species. LiHMDS acts as stoichiometric base and polymerization catalyst.

Table 2. SEC characterization of **PB''** polymers obtained from polymerization of **20**.

Polymer	$[M]_0/[I]$	LiHMDS x [I]	$M_{n,theor}$ (kDa)	$M_{n,GPC}$ (kDa)	\bar{D}	$[\alpha]_D^{25}$	Yield	Conversion
PB1''	12	2.5	5.6	6.0	1.1	+30.7°	75%	100%
PB2''	25	2.5	11.7	13.2	1.1	+21.6°	80%	99%
PB3''	50	2.5	23.4	21.7	1.1	+16.1°	74%	98%
PB4''	100	2.5	46.8	38.9	1.1	n.d.	62%	95%

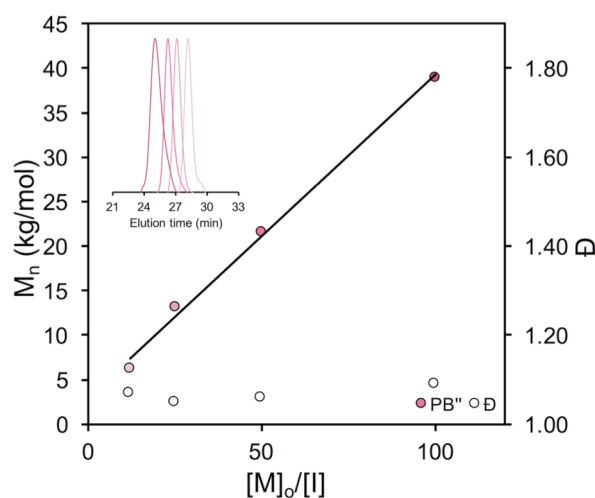


Figure 3. M_n vs. $[M]_0/[I]$ for **PB''** polymers (monomer **20**) indicates linearity up to $[M]_0/[I] = 100$ and dispersities remain under 1.1. Inset shows SEC chromatograms of polymers.

thiophenol and potassium carbonate, and this was explored as an avenue to further reduce the steric constraints of this monomer (Scheme 5). Indeed, when comparing minimized geometries of these monomers (B3LYP/6-31G(d)) in Figure 2, the distance from the lactam nitrogen to the nearest atom is as low as 3.530 Å for the *N*-(2-nitrobenzenesulfonyl)-*N*-boc protected monomer and as high as 5.238 Å for the *N,N*-di-boc protected monomer (Figure S3).

N-nosyl removal reduces β -lactam monomer steric hindrance and facilitates rapid polymerization

In particular, when comparing only the optimized geometries for the *N*-(2-nitrobenzenesulfonyl)-*N*-boc protected and *N*-boc protected monomers, there was a significant increase in the available space in the forward path of polymerization when the nosyl group is not present (3.530 Å to 6.676 Å). Concomitantly, this monomer readily polymerized (Scheme 5, Figure 3, see methods for synthetic details) with molecular weights determined by THF GPC with polystyrene standards ranging from 6.0 kDa to 38.9 kDa as a function of $[M]_0/[I]$ ratio (Table 2).

We observed high polymer conversions greater than 95% as determined by the relative area of the monomer and polymer SEC peaks with catalyst loading of 2.5 x [I] even for the highest molecular weight polymers. The relative reduction in catalyst loading necessary to facilitate complete conversion of monomer **20**, compared to the 3.5 x [I] required for **17**, is likely a result of its reduced steric hindrance. As before, size exclusion chromatograms displayed monomodal distributions with highly narrow \bar{D} of 1.1. To investigate the kinetics of polymerization, we removed aliquots and quenched the polymerization reaction at set time points (20, 40, 60, 90, 120, 180, 240, 300, 1800, 3600 s) from a polymerization reaction with $[M]_0/[I] = 25$ and analyzed the product by SEC. As shown in Figure 4, these intermediate time points of the polymerization showed a peak with high retention time corresponding to the unreacted monomer and a lower retention

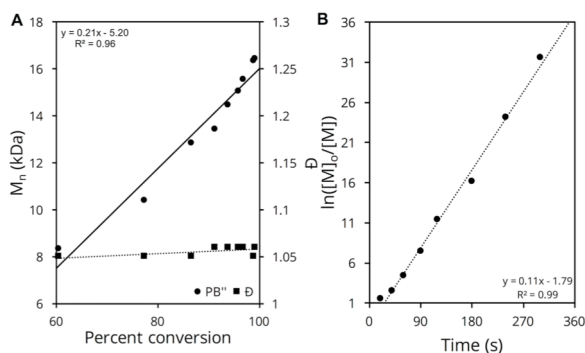


Figure 4. Kinetics of polymerization for monomer **20** are rapid, uniform, and indicate controllability.

time peak corresponding to the growing polymer chain. As polymerization time increased, the calculated area of the monomer peak to the polymer peak decreased from 91.5 to 1.10 $\text{mV} \cdot \text{min}$ as the monomer was consumed while the polymer peak molecular weight increased from ~ 6 kDa to ~ 17 kDa (Figure S4). Importantly, $>95\%$ conversion occurred rapidly after 15 minutes and suggests the potential for improving the controllability of the reaction by slowing chain propagation kinetics.

Deprotection, isolation, and SEC method optimization of water-soluble AmPAS

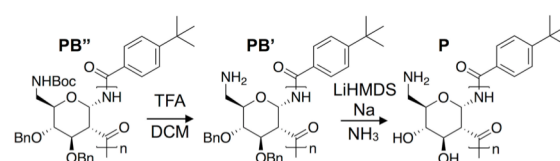
We successfully deprotected these polymers by sequential TFA-mediated Boc removal, isolation of the free base, and Birch-type debenzoylation (Scheme 6, see methods for synthetic details). The water-soluble (stable in solution up to 20 mg/mL) polymers are white, cotton-like solids following dialysis and lyophilization (Table 3). As these polymers are only sparingly soluble in DMF and insoluble in THF, we performed aqueous SEC with poly(2-vinylpyridine) standards to characterize their molecular weight distributions. After an exhaustive SEC buffer optimization (Figure S5), a glycine-acetic acid buffer system at pH 2.3 and total salt concentrations < 120 mM was found to somewhat mitigate these effects. These low pH conditions (< 3) were necessary in order to ensure protonation of the stationary phase to prevent interaction with the polymeric analytes. Additionally, we selected glycine due to its low pKa as well as monovalent charge to prevent crosslinking of our polycationic polymers and reduction of solubility. Finally, acetic acid was necessary to dissolve the poly(2-vinylpyridine) standards for accurate quantification of molecular weight. Under these conditions, experimental M_n were in good agreement with the theoretical M_n prediction and $^1\text{H-NMR}$ end group analysis (Figure S6). Given the known challenges of applying aqueous SEC to the characterization of polyelectrolytes^{51,52}, we were encouraged to find that the calculated dispersities remained ≤ 1.3 even for molecular weights near 10 kDa (Table 3, Figure S7).

AmPAS are water soluble, cationic, and adopt a helical conformation in aqueous solution

Unlike our previously reported glucose- and galactose-derived PAS, the peaks of the $^1\text{H-NMR}$ spectra of AmPAS (**P1-P3**) are broad (Figure S6) and the $^1\text{H}^{13}\text{C-HSQC}$ indicates overlap of the protons of C6 with those of C3 and C2 (Figure S8). Additionally, the ^{13}C NMR spectra of the deprotected polymers show peaks at 170 ppm (amide), 73 ppm (C1), and 51 ppm (C2), confirming the presence of a pyranose ring with amide connectivity (Figure S9). The shift of the C6 carbon, importantly, is 42 ppm which is significantly upfield of the 62 ppm observed for our fully hydroxyl-functionalized glucose PAS²⁰. These data confirm our substitution of the 6'-OH with a less electronegative nitrogen for cationic amine functionality. The presence of cationic primary amines is further supported by a colorimetric titration assay (Figure S10) utilizing Alizarin Yellow R and Thymol Blue, in which the calculated pKa was found to be ~ 10.5 (Figure S10). As such the AmPAS are cationic polymers in aqueous solutions of, for example, pH 7.4.

Despite numerous attempts to vary matrices and concentrations, we only obtained a MALDI-TOF spectrum of **P1**. As expected, the spectrum indicates a monomodal distribution of a singular polymeric species with peak molecular weight of 2.4 kDa uniformly spaced by 189 Da, which is equivalent to the molecular weight of the protonated monomer (189 Da) (Figure S11). IR spectroscopy of the protected polymers confirm the amide bonds and aromatic substituents with peaks at 1690 cm^{-1} , 1530 cm^{-1} , and 700 cm^{-1} . Following complete deprotection, the presence of hydroxyl groups is supported by a broad peak at 3300 cm^{-1} along with a loss of the aromatic peaks at $\sim 700\text{ cm}^{-1}$ (Figure S12).

In all cases, previously published PAS with hydroxyl functionality adopt a helical conformation in solution as supported by CD results, molecular dynamics simulations, and experimental $^1\text{H}^1\text{H-NOESY}$ data³³. As a result, we collected CD spectra of **P1-P3** over a range of pH, temperature, and salt



Scheme 6. Deprotection of **PB''** polymers (see methods): 1) TFA/DCM to remove Boc protecting groups; 2) Birch conditions to remove benzyl protecting groups.

Table 3. SEC characterization of **P** polymers obtained from deprotection of **PB''**.

Polymer	$[M]_0/[I]$	$M_{n,theor}$ (kDa)	$M_{n,NMR}$ (kDa)	$M_{n,GPC}$ (kDa)	$M_{w,GPC}$ (kDa)	$[\alpha]_D^{25}$	\bar{D}	Yield
P1	12	2.6	2.9	4.1	4.7	+98.1°	1.1	41%
P2	25	5.2	6.7	5.6	6.5	+114.7°	1.2	79%
P3	50	10.3	9.4	9.8	13.2	+106.5°	1.3	71%

concentrations to investigate the effect of introducing a cationic

group on the polymer backbone. As shown in Figure 5, the CD spectra of **P1-P3** display a minimum near 220 nm ($[\Theta]_{\text{MRE}} \sim -9 \times 10^3 \text{ deg cm}^2/\text{dmol}$) and a maximum near 190 nm ($[\Theta]_{\text{MRE}} \sim 30 \times 10^3 \text{ deg cm}^2/\text{dmol}$) in agreement with values for intensity and wavelength obtained for the glucose-derived PAS. Negligible differences in both the intensity and wavelength of minima of spectra obtained at pH 3.0 (phosphate buffered) to 7 (phosphate) to 10.0 (borate) indicate that the helical structure remains even as the charge density is dramatically varied from nearly complete protonation at pH 3.0 to ~50% protonation at pH 10.0. Additionally, only a slight decrease in intensity of the minima at 220 nm occurs upon heating **P2** to temperatures as high as 55 °C ($[\Theta]_{\text{MRE}} \sim -7 \times 10^3 \text{ deg cm}^2/\text{dmol}$ to $[\Theta]_{\text{MRE}} \sim -5 \times 10^3 \text{ deg cm}^2/\text{dmol}$) and upon addition of high salt (NaF) and denaturant (urea) concentrations ($[\Theta]_{\text{MRE}} \sim -9 \times 10^3 \text{ deg cm}^2/\text{dmol}$ to $[\Theta]_{\text{MRE}} \sim -7 \times 10^3 \text{ deg cm}^2/\text{dmol}$). These data together indicate that the helical conformation observed in solution is most likely a result of the conformational restriction imposed by the rigid pyranose rings on the ϕ and ψ angles of the amide bond in contrast to the interresidue hydrogen bonding observed for peptides and proteins³³.

Conclusions

Functional polysaccharides obtained from nature, including chitosan, are widely studied as biomaterials and pharmaceuticals despite contamination by chemically similar material, significant batch-to-batch variation, and poorly defined molecular weight distributions. Efforts to address these drawbacks by the chemical synthesis of functional carbohydrate polymers are met by significant synthetic challenges due to the unique chemistry of carbohydrates including the presence of numerous stereocenters, hydroxyl groups requiring protection, and the anomeric effect. The poly-amido-saccharide (PAS) methodology, reported by our group, allows for the high-yielding synthesis of carbohydrate polymers that share many properties with natural polysaccharides including the preservation of stereochemistry, functionalization by hydroxyl groups, and a backbone comprised of pyranose rings. We previously reported cationic AmpPAS with promising biocompatibility and mucoadhesivity, however, due to the constraints of glycal stability, the [2+2] cycloaddition reaction, and polymerization, the synthesis of AmpPAS is not straightforward. Thus, we present a systematic evaluation of synthetic routes and protecting groups suitable for AmpPAS that is also generally applicable to the synthesis of other cationic, water-soluble polymers generated via anionic ring opening polymerization of β -lactam monomers. Specifically, protection of the 6' OH by TIPSCl followed by benzylation and desilylation followed by a Mitsunobu reaction with either *N*-*tert*-butyl-*p*-toluenesulfonamide or *N*-*tert*-butyl-2-nitrobenzenesulfonamide is the most efficient method to arrive at the desired amine-modified glycals. While the lactam forms from the former glycal and polymerizes to molecular weights as high as $M_n \sim 74.8 \text{ kDa}$ with $[M]_0/[I] = 100$, the *N*-tosyl group cannot be deprotected without degrading the carbohydrate backbone. Lactams with *N*-nosyl-*N*-*tert*-butyl protection do not polymerize due

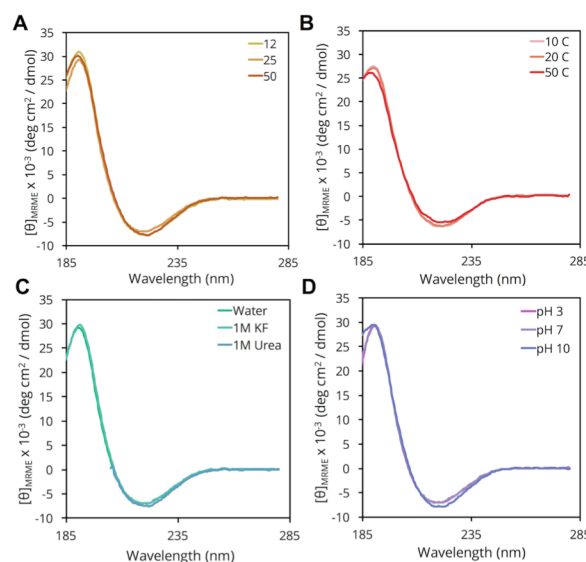


Figure 5. CD spectra of AmpPAS (**P1-P3**) with varying (A): degree of polymerization from 12 to 50; (B): temperature from 10 to 50 °C; (C): salts at high concentration; and, (D): pH from 3 to 10.

to steric considerations, however, removal of the *N*-nosyl group affords a monomer that polymerizes rapidly and controllably with good yields and low \bar{D} . Following deprotection, water soluble carbohydrate polymers are obtained as characterized by NMR, GPC, IR, CD, optical activity, and MALDI-TOF. In solution, these polymers adopt a helical conformation. Continued development of new polymerization methodologies and monomers, such as this one, are in need to address the growing demands for biopolymers and biomaterials in the drug delivery and tissue engineering areas.

Conflicts of interest

There are no conflicts to declare.

Acknowledgements

This work was supported in part by BU and DOD USU (HU0001810012). The authors would like to acknowledge Daniel L. Burke for assistance in synthesizing compounds **11** and **18**, and Dr. Norman C. Lee of the BU Chemical Instrumentation Center for help in obtaining HRMS spectra.

Author Information

Corresponding Author: mgrin@bu.edu

ORCID Numbers

Anant S. Balijepalli	0000-0003-4686-8123
Aladin Hamoud	0000-0001-9928-2906
Mark W. Grinstaff	0000-0002-5453-3668

Notes and references

- 1 D. B. Werz and P. H. Seeberger, Carbohydrates as the Next Frontier in Pharmaceutical Research, *Chem. - A Eur. J.*, 2005, **11**, 3194–3206.
- 2 M. Pogson, G. Georgiou and B. L. Iverson, Engineering next generation proteases, *Curr. Opin. Biotechnol.*, 2009, **20**, 390–397.
- 3 R. J. Williams, Restriction Endonucleases: Classification, Properties, and Applications, *Mol. Biotechnol.*, 2003, **23**, 225–244.
- 4 S. N. Cohen, A. C. Y. Chang, H. W. Boyer and R. B. Helling, Construction of biologically functional bacterial plasmids in vitro, *Proc. Natl. Acad. Sci. U. S. A.*, 1973, **70**, 3240–3244.
- 5 J. M. Palomo, Solid-phase peptide synthesis: an overview focused on the preparation of biologically relevant peptides, *RSC Adv.*, 2014, **4**, 32658–32672.
- 6 K. Itakura, J. J. Rossi and R. B. Wallace, Synthesis and Use of Synthetic Oligonucleotides, *Annu. Rev. Biochem.*, 1984, **53**, 323–356.
- 7 T. J. Boltje, T. Buskas and G.-J. Boons, Opportunities and challenges in synthetic oligosaccharide and glycoconjugate research, *Nat. Chem.*, 2009, **1**, 611–622.
- 8 C. R. Becer, The Glycopolymer Code: Synthesis of Glycopolymers and Multivalent Carbohydrate-Lectin Interactions, *Macromol. Rapid Commun.*, 2012, **33**, 742–752.
- 9 M. H. Caruthers, Gene synthesis machines: DNA chemistry and its uses, *Science (80-.)*, 1985, **230**, 281–285.
- 10 R. Xiao and M. W. Grinstaff, Chemical synthesis of polysaccharides and polysaccharide mimetics, *Prog. Polym. Sci.*, 2017, **74**, 78–116.
- 11 P. Stallforth, B. Lepenies, A. Adibekian and P. H. Seeberger, Carbohydrates: A frontier in medicinal chemistry, *J. Med. Chem.*, 2009, **52**, 5561–5577.
- 12 G. A. Paredes-Juarez, B. J. de Haan, M. M. Faas and P. de Vos, A technology platform to test the efficacy of purification of alginate, *Materials (Basel)*, 2014, **7**, 2087–2103.
- 13 S. K. Tam, J. Dusseault, S. Polizu, M. Ménard, J. P. Hallé and L. Yahia, Impact of residual contamination on the biofunctional properties of purified alginates used for cell encapsulation, *Biomaterials*, 2006, **27**, 1296–1305.
- 14 R. Lieder, V. S. Gaware, F. Thormodsson, J. M. Einarsson, C. H. Ng, J. Gislason, M. Masson, P. H. Petersen and O. E. Sigurjonsson, Endotoxins affect bioactivity of chitosan derivatives in cultures of bone marrow-derived human mesenchymal stem cells, *Acta Biomater.*, 2013, **9**, 4771–4778.
- 15 M. Stefansson, Assessment of alginic acid molecular weight and chemical composition through capillary electrophoresis, *Anal. Chem.*, 1999, **71**, 2373–2378.
- 16 R. H. Chen, J. R. Chang and J. S. Shyr, Effects of ultrasonic conditions and storage in acidic solutions on changes in molecular weight and polydispersity of treated chitosan, *Carbohydr. Res.*, 1997, **299**, 287–294.
- 17 S. Bertini, A. Bisio, G. Torri, D. Bensi and M. Terbojevich, Molecular weight determination of heparin and dermatan sulfate by size exclusion chromatography with a triple detector array, *Biomacromolecules*, 2005, **6**, 168–173.
- 18 S. Ha, J. Gao, B. Tidor, J. W. Brady and M. Karplus, Solvent Effect on the Anomeric Equilibrium in D-Glucose: A Free Energy Simulation Analysis, *J. Am. Chem. Soc.*, 1991, **113**, 1553–1557.
- 19 O. Calin, S. Eller and P. H. Seeberger, Automated polysaccharide synthesis: Assembly of a 30mer mannoside, *Angew. Chemie - Int. Ed.*, 2013, **52**, 5862–5865.
- 20 E. L. Dane and M. W. Grinstaff, Poly-amido-saccharides: Synthesis via Anionic Polymerization of a β -Lactam Sugar Monomer, *J. Am. Chem. Soc.*, 2012, **134**, 16255–16264.
- 21 Y. Koda, T. Terashima and M. Ouchi, Unnatural Oligoaminosaccharides with N-1,2-Glycosidic Bonds Prepared by Cationic Ring-Opening Polymerization of 2-Oxazoline-Based Heterobicyclic Sugar Monomers, *ACS Macro Lett.*, 2019, 1456–1460.
- 22 P. Yadav, H. Yadav, V. G. Shah, G. Shah and G. Dhaka, Biomedical Biopolymers, their Origin and Evolution in Biomedical Sciences: A Systematic Review., *J. Clin. Diagn. Res.*, 2015, **9**, ZE21-5.
- 23 M. Fernández-García and A. Muñoz-Bonilla, Hybrid Glycopolymer Materials and Their Expansive Applications, *Glycopolymer Code Synth. Glycopolymers their Appl.*, 2015, 221–256.
- 24 G. Coullerez, P. H. Seeberger and M. Textor, Merging Organic and Polymer Chemistries to Create Glycomaterials for Glycomics Applications, *Macromol. Biosci.*, 2006, **6**, 634–647.
- 25 A. Basu, K. R. Kunduru, E. Abteu and A. J. Domb, Polysaccharide-Based Conjugates for Biomedical Applications, *Bioconjug. Chem.*, 2015, **26**, 1396–1412.
- 26 L.-S. Liu, S.-Q. Liu, S. Y. Ng, M. Froix, T. Ohno and J. Heller, Controlled release of interleukin-2 for tumour immunotherapy using alginate/chitosan porous microspheres, *J. Control. Release*, 1997, **43**, 65–74.
- 27 G. D. Monheit and K. M. Coleman, Hyaluronic acid fillers, *Dermatol. Ther.*, 2006, **19**, 141–150.
- 28 A. D. Augst, H. J. Kong and D. J. Mooney, Alginate Hydrogels as Biomaterials, *Macromol. Biosci.*, 2006, **6**, 623–633.
- 29 R. Jayakumar, D. Menon, K. Manzoor, S. V Nair and H. Tamura, Biomedical applications of chitin and chitosan based nanomaterials - A short review, *Carbohydr. Polym.*, 2010, **82**, 227–232.
- 30 S. Fu, A. Thacker, D. M. Sperger, R. L. Boni, S. Velankar, E. J. Munson and L. H. Block, Rheological evaluation of inter-grade and inter-batch variability of sodium alginate, *AAPS PharmSciTech*, 2010, **11**, 1662–1674.
- 31 G. A. Morris, J. Castile, A. Smith, G. G. Adams and S. E. Harding, The effect of prolonged storage at different temperatures on the particle size distribution of tripolyphosphate (TPP)-chitosan nanoparticles, *Carbohydr. Polym.*, 2011, **84**, 1430–1434.

- 32 E. L. Dane, S. L. Chin and M. W. Grinstaff, Synthetic Enantiopure Carbohydrate Polymers That Are Highly Soluble in Water and Noncytotoxic, *ACS Macro Lett.*, 2013, **2**, 887–890.
- 33 S. L. Chin, Q. Lu, E. L. Dane, L. Dominguez, C. J. McKnight, J. E. Straub and M. W. Grinstaff, Combined Molecular Dynamics Simulations and Experimental Studies of the Structure and Dynamics of Poly-Amido-Saccharides, *J. Am. Chem. Soc.*, 2016, **138**, 6532–6540.
- 34 Y.-Y. T. Tsao and K. L. Wooley, Synthetic, Functional Thymidine-Derived Polydeoxyribonucleotide Analogues from a Six-Membered Cyclic Phosphoester, *J. Am. Chem. Soc.*, 2017, **139**, 5467–5473.
- 35 T. P. Gustafson, A. T. Lonnecker, G. S. Heo, S. Zhang, A. P. Dove and K. L. Wooley, Poly(d-glucose carbonate) block copolymers: A platform for natural product-based nanomaterials with solvothermic characteristics, *Biomacromolecules*, 2013, **14**, 3346–3353.
- 36 A. T. Lonnecker, Y. H. Lim and K. L. Wooley, Functional Polycarbonate of a d-Glucal-Derived Bicyclic Carbonate via Organocatalytic Ring-Opening Polymerization, *ACS Macro Lett.*, 2017, **6**, 748–753.
- 37 L. Li, K. Knickelbein, L. Zhang, J. Wang, M. Obrinske, G. Z. Ma, L. M. Zhang, L. Bitterman and W. Du, Amphiphilic sugar poly(orthoesters) as pH-responsive nanoscopic assemblies for acidity-enhanced drug delivery and cell killing, *Chem. Commun.*, 2015, **51**, 13078–13081.
- 38 L. Li, J. Wang, M. Obrinske, I. Milligan, K. O'Hara, L. Bitterman and W. Du, Syntheses of sugar poly(orthoesters) through reverse anomeric effect, *Chem. Commun.*, 2015, **51**, 6972–6975.
- 39 M. Metzke, N. O'Connor, S. Maiti, E. Nelson and Z. Guan, Saccharide-Peptide Hybrid Copolymers as Biomaterials, *Angew. Chemie Int. Ed.*, 2005, **44**, 6529–6533.
- 40 V. Ladmiral, E. Melia and D. M. Haddleton, Synthetic glycopolymers: an overview, *Eur. Polym. J.*, 2004, **40**, 431–449.
- 41 R. Xiao, E. L. Dane, J. Zeng, C. J. McKnight and M. W. Grinstaff, Synthesis of Altrose Poly-amido-saccharides with β -N-(1 \rightarrow 2)-d-amide Linkages: A Right-Handed Helical Conformation Engineered in at the Monomer Level, *J. Am. Chem. Soc.*, 2017, **139**, 14217–14223.
- 42 E. L. Dane, A. E. Ballok, G. A. O'Toole and M. W. Grinstaff, Synthesis of Bioinspired Carbohydrate Amphiphiles that Promote and Inhibit Biofilms., *Chem. Sci.*, DOI:10.1039/C3SC52777H.
- 43 K. Zhang, Y. Du, Z. Si, Y. Liu, M. E. Turvey, C. Raju, D. Keogh, L. Ruan, S. L. Jothy, S. Reghu, K. Marimuthu, P. P. De, O. T. Ng, J. R. Mediavilla, B. N. Kreiswirth, Y. R. Chi, J. Ren, K. C. Tam, X. W. Liu, H. Duan, Y. Zhu, Y. Mu, P. T. Hammond, G. C. Bazan, K. Pethe and M. B. Chan-Park, Enantiomeric glycosylated cationic block co-beta-peptides eradicate *Staphylococcus aureus* biofilms and antibiotic-tolerant persisters, *Nat. Commun.*, 2019, **10**, 4792.
- 44 I. A. Sogias, A. C. Williams and V. V. Khutoryanskiy, Why is Chitosan Mucoadhesive?, *Biomacromolecules*, 2008, **9**, 1837–1842.
- 45 W. E. Rudzinski and T. M. Aminabhavi, Chitosan as a carrier for targeted delivery of small interfering RNA, *Int. J. Pharm.*, 2010, **399**, 1–11.
- 46 A. S. Balijepalli, R. C. Sabatelle, M. Chen, B. Suki and M. W. Grinstaff, A Synthetic Bioinspired Carbohydrate Polymer with Mucoadhesive Properties, *Angew. Chemie*, DOI:10.1002/anie.201911720.
- 47 V. Basava, S. M. Gorun and C. H. Marzabadi, An improved synthesis of 3,6-anhydro-d-glucal and a study of its unusual chemical reactivity, *Carbohydr. Res.*, 2014, **391**, 106–111.
- 48 S. Fletcher, The Mitsunobu reaction in the 21st century, *Org. Chem. Front.*, 2015, **2**, 739–752.
- 49 Z. Kaluza and M. Chmielewski, Synthesis of 1-oxabicyclic β -lactam precursors from 4,6-O-benzylidene-D-allal, *Tetrahedron*, 1989, **45**, 7195–7200.
- 50 M. Chmielewski, Z. Kaluza and B. Furman, Stereocontrolled synthesis of 1-oxabicyclic β -lactam antibiotics via [2 + 2]cycloaddition of isocyanates to sugar vinyl ethers, *Chem. Commun.*, 1996, 2689–2696.
- 51 I. J. Levy and P. L. Dubin, Molecular Weight Distributions of Cationic Polymers by Aqueous Gel Permeation Chromatography, *Ind. Eng. Chem. Prod. Res. Dev.*, 1982, **21**, 59–63.
- 52 H. Xing, M. Lu, L. Xian, J. Zhang, T. Yang, L. Yang and P. Ding, Molecular weight determination of a newly synthesized guanidynylated disulfide-containing poly(amido amine) by gel permeation chromatography, *Asian J. Pharm. Sci.*, 2017, **12**, 292–298.

We expand the scope of the PAS methodology and evaluate multiple synthetic routes to generate a regioselectively-functionalized 6-amino carbohydrate polymer sharing key properties with natural polysaccharides, including high water-solubility.

